NASA TECHNICAL MEMORANDUM 107616

A MICROMECHANICS-BASED STRENGTH PREDICTION METHODOLOGY FOR NOTCHED METAL MATRIX COMPOSITES

C. A. Bigelow

APRIL 1992

Presented at Fatigue and Fracture of Inorganic Composites, Churchill College, Cambridge, UK, March 31-April 2, 1992

National Aeronautics and
Space Administration

Langley Research Center
Hampton, Virginia 23665

ABSTRACT

An analytical micromechanics-based strength prediction methodology was developed to predict failure of notched metal matrix composites. The stress-strain behavior and notched strength of two metal matrix composites, boron/aluminum (B/Al) and silicon-carbide/titanium (SCS-6/Ti-15-3), were predicted. The prediction methodology combines analytical techniques ranging from a three-dimensional finite-element analysis of a notched specimen to a micromechanical model of a single fiber. In the B/Al laminates, a fiber failure criterion based on the axial and shear stress in the fiber accurately predicted laminate failure for a variety of layups and notch-length-to-specimen-width ratios with both circular holes and sharp notches when matrix plasticity was included in the analysis. For the SCS-6/Ti-15-3 laminates, a fiber failure based on the axial stress in the fiber correlated well with experimental results for static and post-fatigue residual strengths when fiber-matrix debonding and matrix cracking were included in the analysis. The micromechanics-based strength prediction methodology offers a direct approach to strength predictions by modeling behavior and damage on a constituent level, thus, explicitly including matrix nonlinearity, fiber-matrix interface debonding and matrix cracking.

INTRODUCTION

Metal matrix composites (MMCs) have several inherent properties, such as high stiffness-to-weight ratios and high strength-to-weight ratios, which make them attractive for advanced aerospace applications. These composites also have a higher operating temperature range than polymer matrix composites. Like polymer composites, MMCs are very notch sensitive. The degree of notch sensitivity depends on notch size and shape, laminate orientation and material properties. Fiber-matrix interfaces can also play a key role in the mechanical behavior of MMCs[1]. The interfaces govern the mode and extent of load transfer between the fiber and matrix. When the interfaces are strong and transmit all loads fully, isolated fiber fractures tend to spread more rapidly to other fibers and hasten failure[2]. To design damage-tolerant structures, or to simply understand the effects of fastener holes, the laminate fracture strength must be known for a wide range of laminates, notch geometries, loading conditions, and material properties. To avoid testing all possible parametric combinations, an analytical method for predicting the fracture strength of notched MMCs is needed.

Over the past decade, researchers at NASA Langley Research Center have analyzed a number of notched MMC laminates for a variety of behaviors and have developed an analytical micromechanics-based strength prediction methodology to predict failure of notched MMCs. This paper will review the analytical methodology and present selected results. The micromechanics-based strength prediction methodology combines analytical techniques ranging from a three-dimensional (3D)

orthotropic finite element (FE) model of a notched specimen to a micromechanical model of a single fiber. Work with B/Al MMCs showed that in this low yield strength matrix, extensive yielding of the matrix occurred at the notch tips, such that specimens with sharp notches and center holes failed at similar stress levels[3]. In brittle polymeric matrix composites, similar notch insensitive results have been observed for quasi-isotropic laminates[4]. However, in polymeric composites, the notch-insensitivity was caused by extensive matrix cracking and delaminations near the crack tip that significantly reduced the local stress concentration[5]. The fiber-matrix interface plays a particularly significant role in MMCs with a matrix having a high yield strength, such as silicon-carbide/titanium (SCS-6/Ti-15-3). Debonding of the fiber-matrix interface was found to be a primary damage mechanism in SCS-6/Ti-15-3 composites[1]. Extensive fiber-matrix debonding occurred such that specimens with sharp notches and center holes failed at similar stress levels[6]. Matrix cracking was found to be a significant factor in predicting the post-fatigue residual strength of SCS-6/Ti-15-3 specimens containing center holes[7].

Traditional strength prediction approaches do not lend themselves to MMCs when highly nonlinear behavior is observed or when excessive matrix damage (i.e., fiber-matrix debonding, matrix cracking) proceeds laminate failure. For example, linear elastic fracture mechanics (LEFM) methods, (see, for example, work by Waddoups, Eisenmann, and Kaminski[8]) would not apply when the material behaves nonlinearly. A LEFM approach could possibly be used in cases of matrix damage without material nonlinearity but this would require orthotropic stress-intensity factor solutions for extremely complex crack configurations. The two-parameter approaches, such as introduced by Whitney and Nuismer[9,10], use elastic stress solutions for undamaged configurations and attempt to account for damage through the use of some characteristic length. (An extensive review of commonly used fracture models for predicting the notched strength of composite laminates is presented elsewhere[11].) The new micromechanics-based strength prediction methodology described herein presents a more direct approach by modeling behavior and damage on a constituent level, thus, accounting for the matrix nonlinearity, fiber-matrix interface debonding and matrix cracking.

The following sections will briefly describe the prediction methodology and present results for notched metal matrix composites.

MICROMECHANICS-BASED STRENGTH PREDICTION METHODOLOGY

The micromechanics-based strength prediction methodology developed at NASA Langley is based on constituent level behavior and combines three analytical techniques to predict various aspects of the specimen and material behavior of notched MMCs. The first analytical technique, a three-dimensional (3D) finite element (FE) analysis (PAFAC[12]), was used to analyze the global behavior of notched specimens with and without damage. The second, a discrete fiber-matrix (DFM) finite element model was used to analyze fiber-matrix interface stresses. The

third, a macro-micromechanical analysis (MMA)[13], combines the 3D FE analysis with the unit cell DFM model. The MMA was used to analyze notch-tip stress states in notched configurations with no damage. In all cases, the bulk matrix properties were obtained from matrix material that was subjected to the same processing cycles as the composite laminates[1,3].

Three-Dimensional Analysis, PAFAC

The overall specimen behavior was analyzed with a three-dimensional finite element program called PAFAC[12], which was developed from a program written by Bahei-El-Din[14,15]. PAFAC (Plastic and Failure Analysis of Composites) uses a constant strain, eight-noded, hexahedral element. Each hexahedral element represents a unidirectional composite material whose fibers can be oriented in the appropriate direction in the structural (Cartesian) coordinate system. The PAFAC program uses the vanishing-fiber-diameter (VFD) material model developed by Bahei-El-Din and Dvorak[14,16,17] to model the elastic-plastic matrix and elastic fiber based on the constituent properties. Either the Ramberg-Osgood equation[18] or a piece-wise linear approximation may be used to model the nonlinear stress-strain curve of the matrix. The fiber is modeled as an linear-elastic material. The PAFAC program predicts fiber and matrix stresses at each element centroid. Using this material model, the analysis calculates the fiber and laminate stresses and predicts when yielding occurs in each element of the finite element mesh.

The program PAFAC was used to predict the laminate behavior and first fiber failure. PAFAC predicts first fiber failure to occur when the fiber stresses within an element exceed a given criterion. For the analysis of the B/Al composites[3], a fiber failure criterion based on the axial and shear stress in the fiber was used. Due to limited computer resources available at the time, the elements at the notch tip were approximately three fibers wide in the FE meshes used to analyze the B/Al laminates. Thus, "first fiber failure" actually indicated failure of all three fibers within an element in the B/Al analyses. In later work[6,7], meshes were refined so that the smallest elements, located next to the notch or hole, were one fiber spacing wide. The appropriate fiber spacing was calculated using the composite fiber volume fraction, the fiber diameter, and the ply thickness. For the analyses of titanium MMCs[6,7], a fiber failure criterion based on the axial stress in the fiber was used.

Tests of unnotched SCS-6/Ti-15-3 laminates[1] indicated interfacial debonding in the 90^{o} plies at applied stresses that were as low as 20% of the yield strength of the matrix. To account for the debonding, the PAFAC analysis was modified to include a failure criterion to approximate interfacial debonding in the 90^{o} plies. When the transverse stress in the elements in the 90^{o} plies reached a specified critical value, the material properties of the 90^{o} plies were modified to represent a ply with a completely debonded interface. For the SCS-6/Ti-15-3 material, the critical transverse stress was chosen to be 155 MPa based on the observed stress-strain behavior of unnotched $[90]_8$ laminates[1].

The PAFAC analysis was also modified to account for interface debonding in the 0^o plies at the notch tip in a specimen with a sharp notch[6]. The FE meshes were designed to contain one layer of elements per ply where the elements at the notch tip were one fiber spacing wide. The elements next to the notch tip, which were one fiber spacing wide, were modified to include isotropic layers next to the notch and between each ply. To model the fiber-matrix debonding of the 0^o fiber next to the notch, the elastic modulus of the additional isotropic elements in both 0^o plies was reduced. The remaining elements in the 0^o plies were modeled as composite elements with appropriately higher fiber volume fractions. Various debond lengths of the 0^o fiber were modeled by reducing the modulus of increasing numbers of elements.

Discrete Fiber-Matrix Model

A discrete fiber-matrix (DFM) model (often referred to as a unit cell model) assuming an infinitely repeating, rectangular array of fibers was used to analyze a single fiber and the surrounding matrix. The MSC/NASTRAN finite element code[19] was used to analyze the DFM model using three-dimensional, eight-noded, hexahedral elements. A piece-wise linear approximation of the matrix stress-strain curve was used to model the nonlinear behavior of the matrix and the fiber was modeled as a linear-elastic material. The ply thickness, the fiber volume fraction, and the fiber diameter were used to calculate the dimensions of the DFM model. Compatibility with adjacent unit cells was enforced by constraining the displacements normal to each face to be equal.

Macro-Micromechanical Analysis (MMA)

The third analytical technique, the macro-micromechanical analysis (MMA), was developed recently by the author[13] and was used to analyze notch-tip stress states in notched configurations. The macro-micromechanical analysis combines the 3D homogeneous, orthotropic finite element analysis (PAFAC) of the notched specimen and the discrete fiber-matrix (DFM) micromechanics model of a single fiber. The MMA was used to calculate the stresses in the notch-tip element in the interior 0^o ply of $[0/90]_{2s}$ laminates assuming a perfectly bonded fiber-matrix interface. The interior 0^o ply was the location of the highest fiber axial stress predicted by the PAFAC analyses of the specimens. As mentioned, the PAFAC finite element mesh was designed so that the dimensions of the elements next to the notch corresponded to a single fiber spacing. A schematic view of the macro-micro interface for a notched specimen is shown in Figure 1. Displacement boundary conditions from the PAFAC analysis are applied to the DFM mesh to simulate the stress state next to the notch. The MMA analysis assumes an undamaged composite.

RESULTS AND DISCUSSION

Boron/Aluminum

A wide range of laminates containing both circular holes and sharp notches were tested statically until failure[3]. It was found that, due to widespread yielding of the matrix, specimens with the same notch-length-to-specimen-width ratios (2a/W) failed at similar stress levels.

PAFAC was used to characterize the elastic-plastic behavior of B/Al laminates[3]. The stress-strain curve of the aluminum was modeled with a Ramberg-Osgood equation[18]. The program predicted the stress-strain response for a variety of laminates containing center holes and sharp notches and predicted laminate failure based on the fiber stress in the element next to the notch. The yield pattern of the aluminum matrix material was predicted by the PAFAC program. Since PAFAC is a 3D analysis, yield patterns were predicted for each ply in a multi-ply laminate. Figure 2 shows the yield pattern for a B/Al $[0/\pm45]_S$ laminate with a 25.4-mm-diameter center hole, 2a/W = 0.25 and a fiber volume fraction of 45%. The sketches show the extent of the yielding in the 0^o and 45^o plies as the applied stress is increased. The yielding in the -45^o was very similar to the pattern shown for the 45^o layer. The $\pm45^o$ layers yielded much earlier in the loading history than the 0^o layer. Although not shown, the entire specimen (all plies) had yielded at 150 MPa, 56% of the failure stress. As is typical with a low yield strength matrix, widespread yielding occurred before fiber or specimen failure. In unidirectional B/Al laminates containing circular holes or sharp notches, progressive fiber failures were observed and ,thus, first fiber failure did not correspond to laminate failure. For unidirectional specimens, PAFAC predictions of first fiber failure corresponded to the experimental observations of first fiber failure. In B/Al specimen containing cross-plies ($[\pm45]_{2s}$, $[0/\pm45]_s$, $[0_2/\pm45]_s$), the observed first fiber failure corresponded with laminate failure. Excellent correlation was found between predicted first fiber failure and specimen failure for B/Al laminates containing cross-plies with either circular holes or sharp notches[3]. A typical result is shown in Figure 3, where the applied laminate stress is plotted against the specimen overall strain for a $[0/\pm45]_s$ laminate containing a center hole. The solid line represents the predicted response up to first fiber failure and the symbols represent the experimental results.

Silicon-Carbide/Titanium

Two specimen configurations of a $[0/90]_{2s}$ SCS-6/Ti-15-3 material were tested: a center hole (CH) specimen and a double edge notch (DEN) specimen. The laminate had a fiber volume fraction v_f of 39%. The two specimen configurations failed at similar stress levels in spite of large differences in their stress concentration factors. The elastic stress concentrations K_T are 3.7 for the CH specimen and 5.7 for the DEN specimen[6]. The static strength of the DEN specimen was 520 MPa, for the CH specimen the static strength was 501 MPa. These strengths were unexpectedly close given the difference in the K_T's. Fractographs of the failure surfaces next to the notch for both specimen configurations showed

a fiber-matrix debond length in the notch-tip 0^o fiber of three to four fiber diameters in the DEN specimen, while significant fiber-matrix debonding in the 0^o ply was not present in the CH configuration[6].

The MMA was used to analyze the stresses in the notch-tip element in the interior 0^o ply in both the DEN and CH specimens to determine the fiber-matrix interface stress state. For a unit applied stress (S = 1 MPa), the MMA predicted the s_{rr} stresses shown in Figure 4 for the DEN and CH specimens. The stresses presented are the stresses in the matrix at the fiber-matrix interface calculated at the finite element nodal points. For comparison, the matrix stresses in the interior 0^o ply in an unnotched $[0/90]_{2s}$ specimen due to a unit applied stress are also shown. The stresses are presented with respect to a cylindrical coordinate system shown. Stresses are shown for the plane of symmetry on the XZ plane, i.e. through the center line of the notch or hole. For the two notched configurations, $\theta = 180^o$ is the side of the fiber next to the notch.

For interfacial failure, the stress component of primary concern is the radial stress. The peak values of the radial matrix stresses due to a remote stress of 1 MPa are 4.5 and .67 MPa for the DEN and CH specimens, respectively. The peak value of the radial stress for the unnotched laminate is -0.17 MPa. The radial stresses for the DEN configuration are tensile for all values of q, whereas for the CH configurations, the radial stresses are tensile only from approximately 110^o to 250^o, and for the unnotched laminate, the radial stresses are compressive for all values of q. Thus, for a given interfacial strength, the interface in the DEN specimen will debond much earlier in the loading history than in the CH specimen. For a given load, the 0^o fibers next to the notch in the DEN specimen are more likely to have debonded than the 0^o fibers next to the hole in the CH specimen.

The PAFAC analysis was used to determine the effect of debonding in the 0^o plies on the notch-tip fiber stress concentrations with debonded 90^o fiber-matrix interfaces. Figure 5 shows the predictions of the 0^o fiber stress in the first element next to the notch as a function of applied stress for the DEN and CH specimens. The horizontal dashed line indicates the assumed fiber strength of 4200 MPa and the two vertical dash-dotted lines show the experimental strengths of the two specimens. The fiber strength was calculated from the strain to failure of an unnotched $[0/90]_{2s}$ coupon (ε_{ult} = 0.0105 mm/mm) multiplied by the fiber modulus (400 GPa). The solid lines indicate the predicted 0^o fiber stress with no debonding in the 0^o plies for the DEN and CH specimens. When the axial stress in the first 0^o fiber was used as a failure criteria, the analysis predicted the strength of the CH specimen to be 490 MPa, within 2% of the observed strength. However, the strength of the DEN specimen was predicted to 320 MPa, significantly lower than the observed strength of 520 MPa. Debonding at the notch tip in the DEN specimen was simulated as described above. The effect of modeling the 0^o debonding in the DEN specimen is also shown in Figure 5. Modeling a 0^o debond

length of 1.75 fiber diameters (dashed line) reduced the fiber stress in the DEN specimen considerably, increasing the predicted strength to 400 MPa. Modeling a 0^{o} debond length of 3.5 fiber diameters caused the 0^{o} fiber stress to drop nearly to the level of the CH configuration. This debond length is in good agreement with the micrographs of the fracture surface[6] and the predicted strength of 500 MPa is in good agreement with the observed strength of 520 MPa. Modeling a 0^{o} debond length of 7.0 or more fiber diameters, the 0^{o} fiber stress in the notch-tip element in DEN specimen was reduced to a level below that of the CH configuration. These results indicate that, as with the cross-ply B/Al laminates, a first fiber failure criteria can accurately predict notched strengths when fracture is sudden and catastrophic with no progressive fiber failures.

The development of fatigue damage in SCS-6/Ti-15-3 laminates containing center holes was also investigated[7]. Although the same composite material was used, the laminate used in the fatigue investigations was slightly different than that used for the static loading previously described. For the fatigue loading studies, a $[0/90]_{S}$ four-ply laminate with a fiber volume fraction of 35.5% was used. Damage progression was monitored at various stages of fatigue loading. In general, fatigue damage consisted of fiber-matrix debonding in the 90^{o} plies with matrix cracks extending from the debonded interfaces. The loading modulus of the composite was reduced by 38% due to the matrix cracking. The matrix cracks observed on the surface were bridged by 0^{o} fibers. No fiber failures were observed due to the fatigue loading.

The post-fatigue residual strength was predicted using the PAFAC program. The 0^{o} fiber axial stress next to the hole was predicted for the undamaged virgin and the post-fatigue damaged conditions as a function of applied load. As before, the laminate strength was assumed to be the applied load at which the axial stress in the 0^{o} fiber next to the hole reached the fiber strength.

The through-the-thickness matrix cracking was modeled in the PAFAC analysis by reducing the matrix modulus by 69%. This reduction in the matrix modulus corresponded to the measured 38% reduction in the composite longitudinal modulus[7]. The reduced matrix modulus was used only for the post-fatigue predictions. As previously mentioned, debonding of the fiber-matrix interfaces in the 90^{o} plies in this composite occurs at relatively low load levels. The debonding of the 90^{o} plies was included in the predictions for the virgin condition by modifying the material properties of the 90^{o} plies as described above.

The post-fatigue residual strength was predicted for a specimen that had been subjected to 200,000 cycles at a load level of 250 MPa. No fiber failures were observed and the matrix cracks had reached a saturated state. Small regions located directly above and below the center hole had developed no matrix cracks. The matrix modulus of the elements in regions where cracking was seen was re-

duced. In the regions where no matrix cracks were seen, the element properties were not changed.

The axial stress in the 0^o fiber next to the center hole as a function of the applied stress is shown in Figure 6. The horizontal line indicates the assumed fiber strength of 4400 MPa and the two vertical lines show the experimental strengths for the two conditions. The fiber strength was calculated from the measured strain to failure of an unnotched $[0/90]_s$ specimen (ε_{ult} = 0.0011) multiplied by the fiber modulus (400 GPa). (The fiber strength determined here is slightly different than determined previously since the laminate used in the fatigue loading is not identical to that used in the static loadings.) As shown in the figure, the applied stress at which the 0^o fiber stress equals the fiber strength corresponds closely to the measured strength for both conditions. Using the axial stress in the 0^o fiber next to the hole as a failure criterion for laminate failure, both predictions are within 8% of the experimental values. Again, the first fiber failure criterion accurately predicted the specimen strength when failure was sudden and catastrophic and no progressive fiber failures were observed.

Thermal Residual Stresses

The calculations presented above did not explicitly include any thermal residual stresses. Thermal residual stresses were not found to be significant in the B/Al laminates[3], however, they had a significant effect on the behavior of the SCS-6/Ti-15-3 laminates[1]. The fiber strengths used in the predictions were determined from unnotched SCS-6/Ti-15-3 laminates which were processed the same as the notched specimens and, therefore, the thermal residual stresses were the same in each laminate tested. The thermal residual stresses were implicitly included in the strength predictions since the fiber strengths were determined including the thermal residual stresses.

CONCLUDING REMARKS

An analytical micromechanics-based strength prediction methodology was developed to predict failure of notched metal matrix composites (MMCs). The prediction methodology combines analytical techniques ranging from a three-dimensional orthotropic finite element model of a notched specimen to a micromechanical model of a single fiber. The stress-strain behavior and failure strengths of two metal matrix composites, boron/aluminum (B/Al) and silicon-carbide/titanium (SCS-6/Ti-15-3), were predicted analytically. Five laminates of B/Al composites containing circular holes and notches were tested and analyzed. Due to widespread yielding of the matrix, specimens with the same notch-length-to-specimen-width ratio failed at similar stress levels. Two specimen configurations of SCS-6/Ti-15-3 laminate were tested and analyzed: a center hole (CH) specimen and a double edge notch (DEN) specimen. Due to fiber-matrix debonding in the 0^o plies, the two specimen configurations failed at similar stress levels in spite of the large difference in the stress concentration factors for the two geometries.

A three-dimensional finite element analysis was used to predict the overall stress-deformation behavior and the notch-tip fiber stresses in the B/Al laminates. The analysis accurately predicted the stress-strain response and laminate failure when matrix plasticity was modeled. In the B/ Al laminates, a fiber failure criterion based on the tensile and shear stress in the fiber accurately predicted laminate failure for a variety of layups and notch-to-width ratios with both circular holes and sharp notches.

Two analytical techniques, the three-dimensional finite element analysis and a macro-micromechanical analysis were used to predict the overall stress-deformation behavior and the notch-tip fiber-matrix interface stresses in notched SCS-6/Ti-15-3 materials. Fiber-matrix debonding in the 0^{o} plies was predicted to occur much earlier in the loading history for the DEN specimen and, for a given stress level, more fiber-matrix debonding was predicted to occur in the DEN specimen than in the CH specimen. The overall stress-deformation response of both specimens was accurately predicted when interfacial failure of the 90^{o} plies was included in the analysis. When the modulus of elements at the notch tip was reduced to simulate the observed debonding next to the notch in the 0^{o} plies, predictions of notch-tip 0^{o} fiber stress for the DEN configuration comparable to that of the fiber stress in the CH configuration, indicating that fiber-matrix debonding in the DEN specimen could reduce the notch-tip stress sufficiently so that both configurations would have similar strengths. When the interfacial debonding of the 90^{o} plies and the notch-tip 0^{o} plies (in the DEN specimen) was modeled, the axial stress in the first intact 0^{o} fiber correlated well with the specimen static strength for both specimen configurations. When matrix fatigue cracks were modeled, the axial stress in the first intact 0^{o} fiber correlated well with the post-fatigue static strength for a CH specimen. A first fiber failure criteria based on the axial stress in the first intact 0^{o} fiber accurately predicted the static strength of notched titanium MMC specimens when interfacial damage was modeled. The post-fatigue residual strength was also accurately predicted by the axial stress in the first intact 0^{o} fiber when matrix cracking was modeled.

Traditional strength prediction approaches do not lend themselves to MMCs when highly nonlinear behavior is observed or when fiber-matrix debonding or matrix cracking proceeds laminate failure. The micromechanics-based strength prediction methodology presented here offers a more direct approach by modeling behavior and damage on a constituent level, thus explicitly modeling matrix nonlinearity, fiber-matrix interface debonding and matrix cracking. Including matrix plasticity in any analysis is not trivial. Predicting interfacial stresses and modeling interfacial failures necessitates great analytical efforts. However, since matrix plasticity, matrix cracking, and fiber-matrix debonding can play such an important role in the behavior of MMCs, this analytical effort is necessary to advance the understanding and prediction of damage initiation and development in MMCs.

REFERENCES

1. Johnson, W. S.; Lubowinski, S. J.; and Highsmith, A. L.: Mechanical Characterization of Unnotched SCS_6/Ti-15-3 Metal Matrix Composites at Room Temperature. *Thermal and Mechanical Behavior of Metal Matrix and Ceramic Matrix Composites, ASTM STP 1080*, J. M. Kennedy, H. H. Moeller, and W. S. Johnson, Eds., American Society for Testing and Materials, Philadelphia, 1990, pp. 193-218.

2. Naik, R. A.; and Pollock, W. D.; and Johnson, W. S.: Effect of a High Temperature Cycle on the Mechanical Properties of Silicon Carbide/Titanium Metal Matrix Composites. *Journal of Materials Science*, Vol. 26, 1991, pp. 2913-2920.

3. Johnson, W. S.; Bigelow, C. A.; and Bahei-El-Din, Y. A.: Experimental and Analytical Investigation of the Fracture Processes of Boron/Aluminum Laminates Containing Notches. NASA TP-2187, National Aeronautics and Space Administration, Washington, DC, 1983.

4. Daniel, I. M.: Failure Mechanisms and Fracture of Composite Laminates with Stress Concentrations. *Proceedings of the VIIth International Conference on Experimental Stress Analysis*, Haifa, Israel, August 23-27, 1982, pp. 1-20.

5. Harris, C. E.; and Morris, D. H.: A Fractographic Investigation of the Influence of Stacking Sequence on the Strength of Notched Laminated Composites. *Fractography of Modern Engineering Materials: Composites and Metals, ASTM STP 948*, J. E. Masters and J. J. Au, Eds., American Society for Testing and Materials, 1987, pp. 131-153.

6. Bigelow , C. A.; and Johnson, W. S.: Effect of Fiber-Matrix Debonding on Notched Strength of Titanium Metal Matrix Composites. NASA TM-104131, August 1991.

7. Bakuckas, J. G., Jr.; Johnson, W. S.; and Bigelow, C. A.: Fatigue Damage in Cross-Ply Titanium Metal Matrix Composites Containing Center Holes. Submitted to *Journal of Engineering and Materials Technology*, Nov. 1991. (Also NASA TM-104197, March 1992)

8. Waddoups, M. E.; Eisenmann, J. R. and Kaminski, B. E.: Macroscopic Fracture Mechanics of Advanced Composite Materials. *Journal of Composite Materials*, Vol. 5, 1971, pp. 446-454.

9. Whitney, J. M. and Nuismer, R. J.: Stress Fracture Criteria for Laminated Composites Containing Stress Concentrations. *Journal of Composite Materials*, Vol. 8, 1974, pp. 253-265.

10. Nuismer, R. J. and Whitney, J. M.: Uniaxial Failure of Composite Laminates Containing Stress Concentrations. *Fracture Mechanics of Composites, ASTM STP 593*, American Society of Testing and Materials, 1975, pp. 117-142.

11. Awerbuch, J. and Madhukar, M. S.: Notched Strength of Composite Laminates: Predictions and Experiments--A Review. *Journal of Reinforced Plastics*, Vol. 4, 1985, pp. 3-159.

12. Bigelow, C. A.; and Bahei-El-Din, Y. A.: Plastic and Failure Analysis of Composites (PAFAC). LAR-13183, COSMIC, University of Georgia, 1983.

13. Bigelow, C. A.; and Naik, R. A: A Macro-Micromechanical Analysis of a Notched Metal Matrix Composite. *Composite Materials, Testing and Design, ASTM STP 1120*, G. Grimes, Ed., American Society for Testing and Materials, Philadelphia, 1992, pp. 222-233.

14. Bahei-El-Din, Y. A.: Plastic Analysis of Metal-Matrix Composite Laminates. Ph.D. Dissertation, Duke University, 1979.

15. Bahei-El-Din, Y. A.; Dvorak, G. J.; and Utku, S.: Finite Element Analysis of Elastic-Plastic Fibrous Composite Structures. *Computers and Structures*, Vol. 13, No. 1-3, June 1981, pp. 321-330.

16. Bahei-El-Din, Y. A.; and Dvorak, G. J.: A Review of Plasticity Theory of Fibrous Composite Materials. *Metal Matrix Composites: Testing, Analysis, and Failure Modes, ASTM STP 1032*, W. S. Johnson, Ed., American Society for Testing and Materials, Philadelphia, 1989, pp. 103-129.

17. Dvorak, G. J.; and Bahei-El-Din, Y. A.: Plasticity Analysis of Fibrous Composites. *Journal of Applied Mechanics*, Vol. 49, 1982, pp. 327-335.

18. Ramberg, W. and Osgood, W. R.: Description of Stress-Strain Curves by Three Parameters. NACA TN 902, 1943.

19. MSC/NASTRAN, Version 6.6, MacNeal-Schwendler Corporation, 1991.

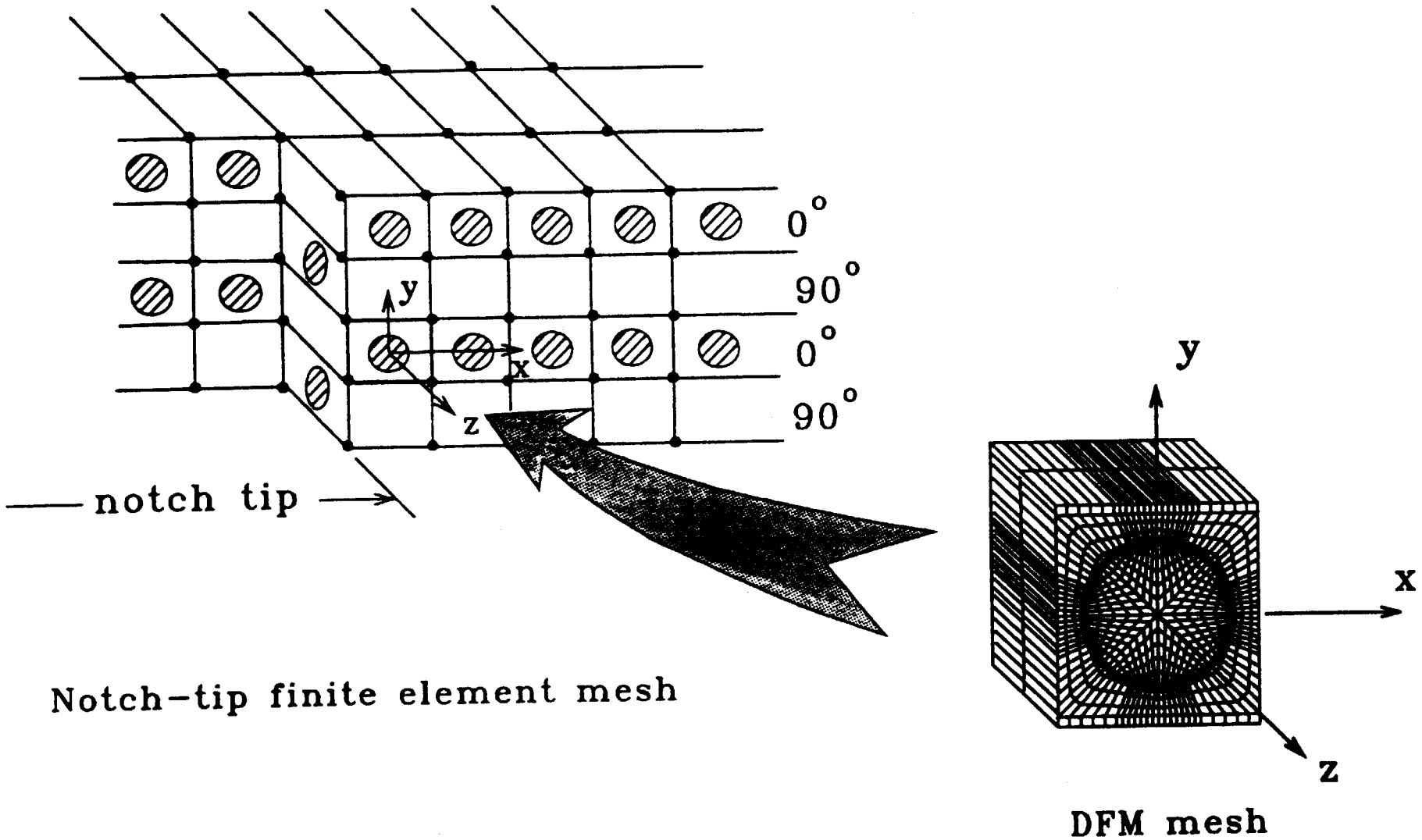

Figure 1. - Schematic of macro-micromehcanical (MMA) interface for double-edge notch specimen.

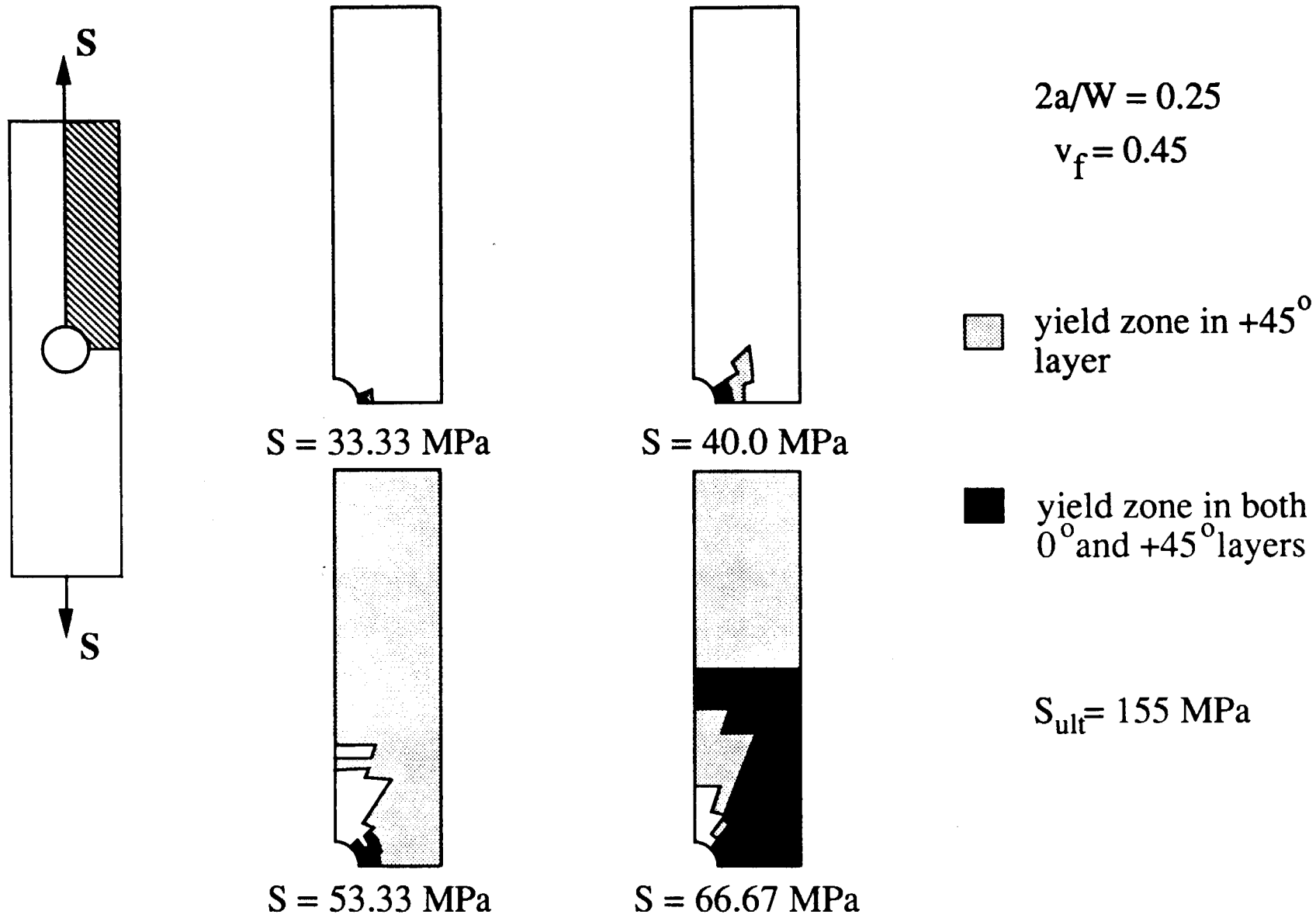

Figure 2. - Yield pattern for $[0/\pm45]_s$ boron/aluminum laminate with center hole.

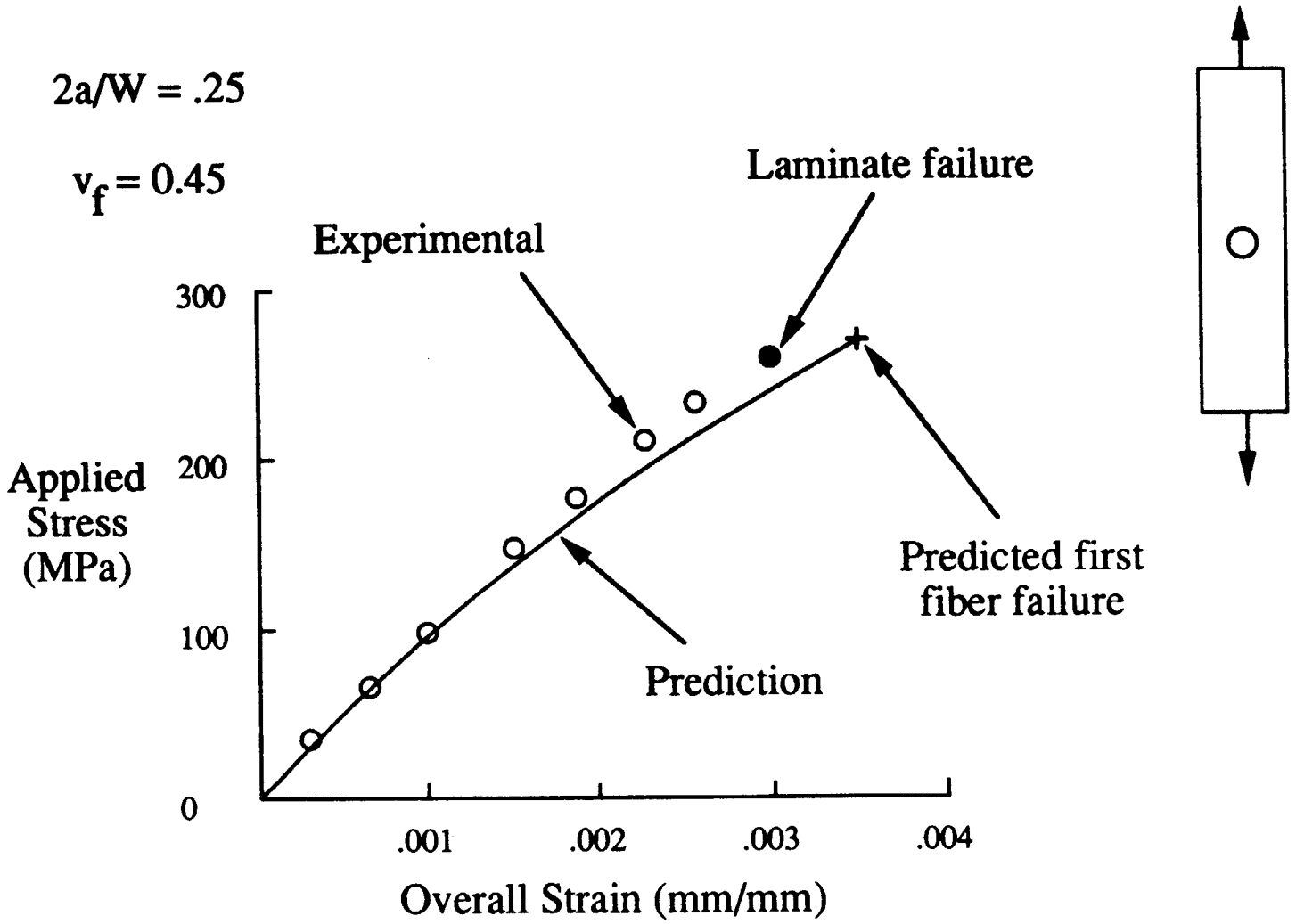

Figure 3. - Stress-strain behavior of $[0/\pm45]_s$ boron/aluminum laminate with center hole.

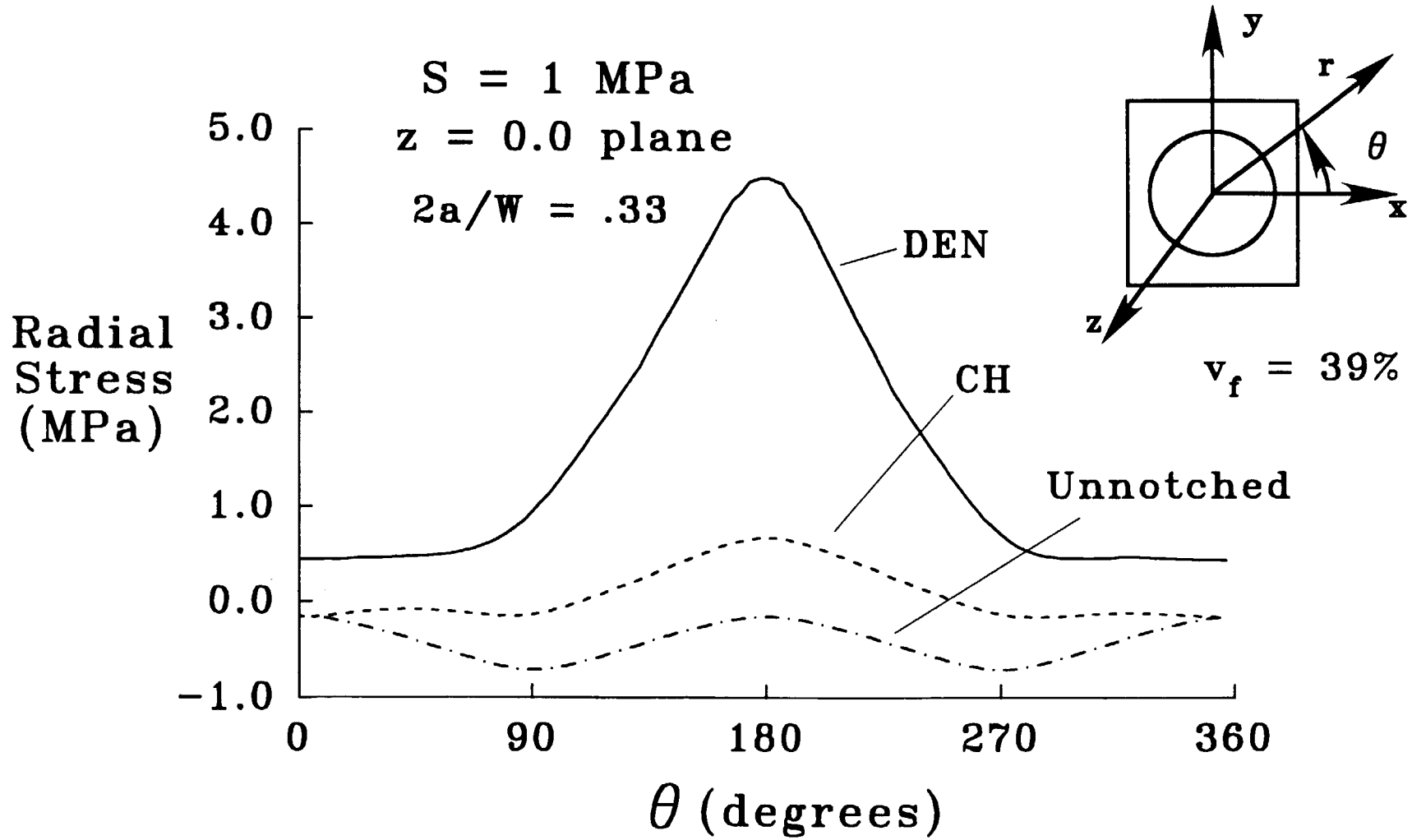

Figure 4. - Radial component of matrix interface stresses for center hole (CH) and double-edge notch (DEN) specimens.

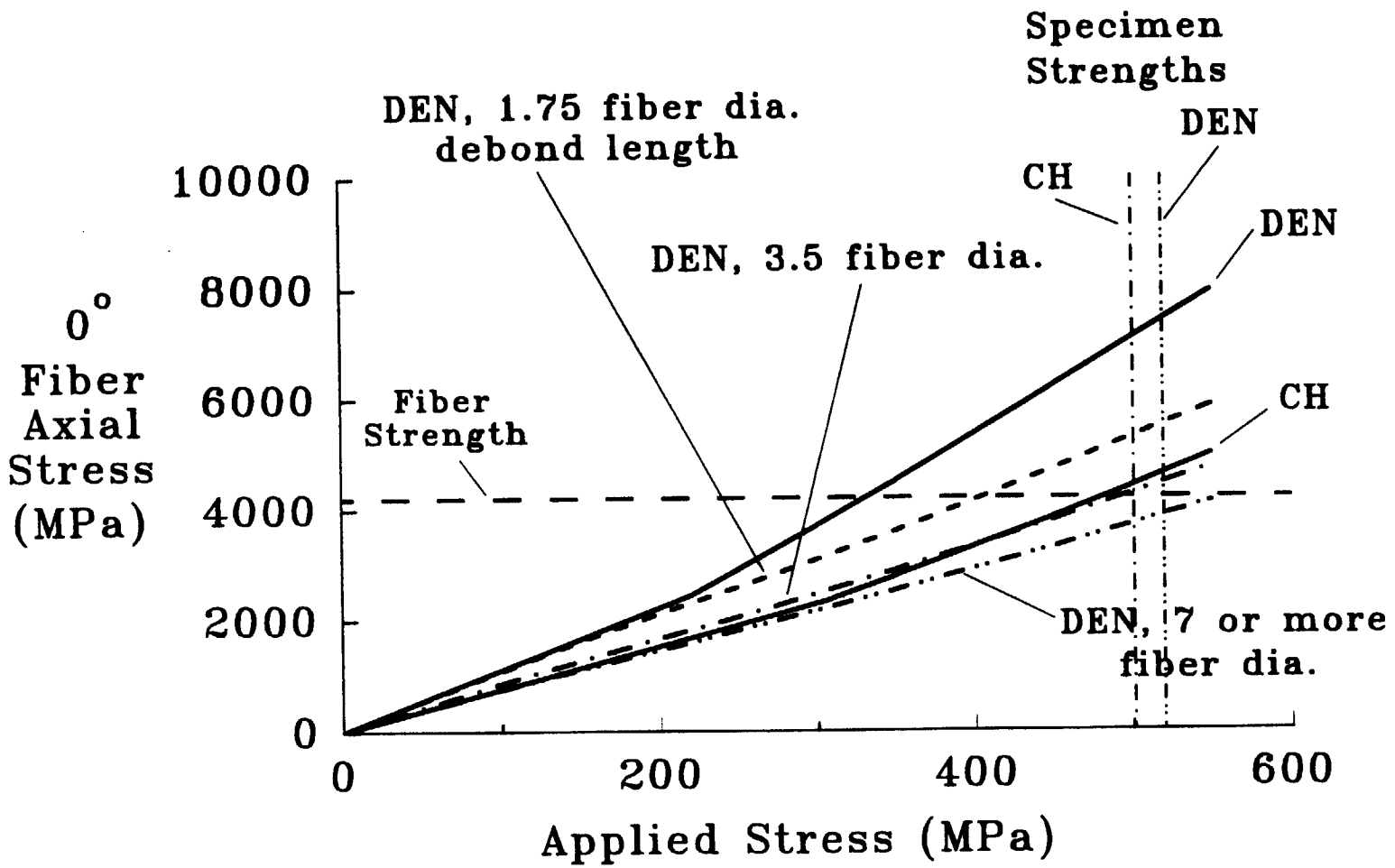

Figure 5. - 0^{o} fiber axial stress for center hole (CH) and double-edge notch (DEN) specimens with notch-tip 0^{o} debonding and debonding of 90^{o} plies. SCS-6/Ti-15-3 $[0/90]_{2s}$, v_f = 39%.

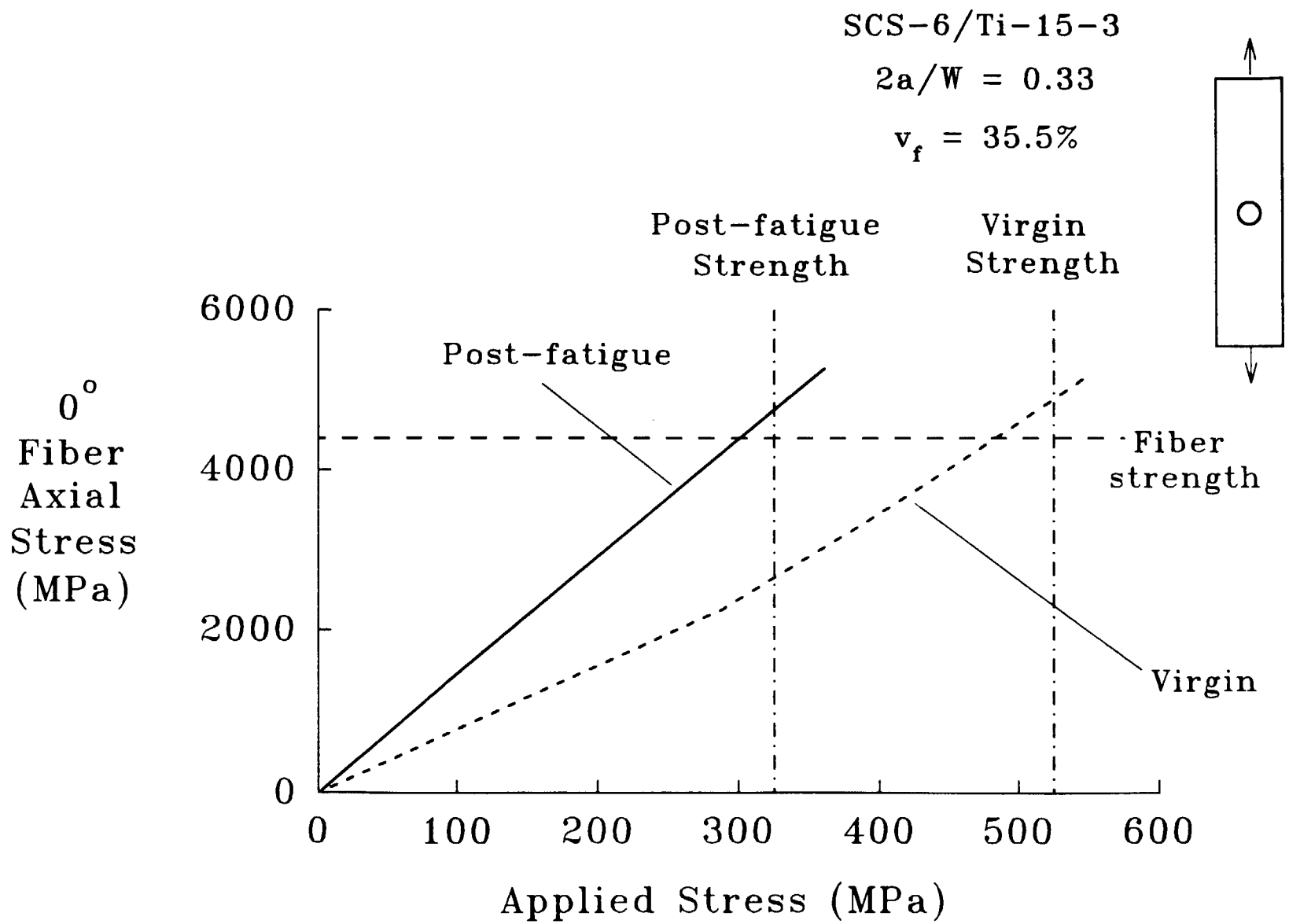

Figure 6. - 0^o axial fiber stress in center hole specimen for virgin and post-fatigue conditions. SCS-6/Ti-15-3 $[0/90]_s$, v_f = 35.5%.

REPORT DOCUMENTATION PAGE

Form Approved
OMB No. 0704-0188

1. AGENCY USE ONLY (Leave blank)	2. REPORT DATE	3. REPORT TYPE AND DATES COVERED
	April 1992	Technical Memorandum

4. TITLE AND SUBTITLE
A Micromechanics-Based Strength Prediction Methodology for Notched Metal Matrix Composites

5. FUNDING NUMBERS
WU 763-23-41-85

6. AUTHOR(S)
C. A. Bigelow

7. PERFORMING ORGANIZATION NAME(S) AND ADDRESS(ES)
NASA Langley Research Center
Hampton, VA 23665-5225

8. PERFORMING ORGANIZATION REPORT NUMBER

9. SPONSORING / MONITORING AGENCY NAME(S) AND ADDRESS(ES)
National Aeronautics and Space Administration
Washington, DC 20546-0001

10. SPONSORING / MONITORING AGENCY REPORT NUMBER
NASA TM-107616

11. SUPPLEMENTARY NOTES

12a. DISTRIBUTION / AVAILABILITY STATEMENT
Unclassified - Unlimited

Subject Category 24

12b. DISTRIBUTION CODE

13. ABSTRACT *(Maximum 200 words)*

An analytical micromechanics-based strength prediction methodology was developed to predict failure of notched metal matrix composites. The stress-strain behavior and notched strength of two metal matrix composites, boron/aluminum (B/Al) and silicon-carbide/titanium (SCS-6/Ti-15-3), were predicted. The prediction methodology combines analytical techniques ranging from a three-dimensional finite-element analysis of a notched specimen to a micromechanical model of a single fiber. In the B/Al laminates, a fiber failure criterion based on the axial and shear stress in the fiber accurately predicted laminate failure for a variety of layups and notch-length-to-specimen-width ratios with both circular holes and sharp notches when matrix plasticity was included in the analysis. For the SCS-6/Ti-15-3 laminates, a fiber failure based on the axial stress in the fiber correlated well with experimental results for static and post-fatigue residual strengths when fiber-matrix debonding and matrix cracking were included in the analysis. The micromechanics-based strength prediction methodology offers a direct approach to strength predictions by modeling behavior and damage on a constituent level, thus, explicitly including matrix nonlinearity, fiber-matrix interface debonding and matrix cracking.

14. SUBJECT TERMS
Boron/aluminum; Silicon-carbide/titanium; Finite-element analysis; Elastic-plastic; Fiber failure

15. NUMBER OF PAGES
18

16. PRICE CODE
A03

17. SECURITY CLASSIFICATION OF REPORT	18. SECURITY CLASSIFICATION OF THIS PAGE	19. SECURITY CLASSIFICATION OF ABSTRACT	20. LIMITATION OF ABSTRACT
Unclassified	Unclassified		